INTERNATIONAL JOURNAL FOR NUMERICAL METHODS IN FLUIDS
Int. J. Numer. Meth. Fluids 2007; **54**:1369–1385
Published online 7 February 2007 in Wiley InterScience (www.interscience.wiley.com). DOI: 10.1002/fld.1434

A stress-based least-squares finite-element model for incompressible Navier–Stokes equations

V. Prabhakar and J. N. Reddy*, †

Department of Mechanical Engineering, Texas A&M University, College Station, TX 77843, U.S.A.

SUMMARY

In this paper we present a stress-based least-squares finite-element formulation for the solution of the Navier–Stokes equations governing flows of viscous incompressible fluids. Stress components are introduced as independent variables to make the system first order. Continuity equation becomes an algebraic equation and is eliminated from the system with suitable modifications. The h and p convergence are verified using the exact solution of Kovasznay flow. Steady flow past a large circular cylinder in a channel is solved to test mass conservation. Transient flow over a backward-facing step problem is solved on several meshes. Results are compared with that obtained using vorticity-based first-order formulation for both benchmark problems. Copyright © 2007 John Wiley & Sons, Ltd.

Received 28 February 2006; Revised 5 December 2006; Accepted 6 December 2006

KEY WORDS: stress-based first-order system; least-squares method; viscous incompressible flow

1. INTRODUCTION

In the past few years finite-element models based on least-squares variational principles have drawn considerable attention for the solution of Stokes and Navier–Stokes equations [1–7]. Least-squares-based finite-element formulations offer several theoretical and computational advantages. Most notably, such formulations circumvent the inf–sup condition of Ladyzhenskaya–Babuska–Brezzi (LBB). As a result equal-order interpolation functions can be used for all field variables.

*Correspondence to: J. N. Reddy, Department of Mechanical Engineering, Texas A&M University, College Station, TX 77843, U.S.A.
†E-mail: jnreddy@tamu.edu

Contract/grant sponsor: Computational Mathematics Program of the Air Force Office of Scientific Research; contract/grant number: F49620-03-1-0201
Contract/grant sponsor: Structural Dynamics Program of Army Research Office; contract/grant number: 45508-EG

They also yield symmetric positive-definite (SPD) coefficient matrix and therefore robust iterative solvers can be used to solve resulting system of algebraic equations.

Vorticity-based least-squares formulation is the most popular first-order formulation for the solution of Stokes and Navier–Stokes equations since only one additional independent variable is introduced in two dimensions compared to three in stress-based formulation and four in velocity–flux formulation. In this paper, we present a stress-based least-squares finite-element formulation that carries five independent variables. In the proposed formulation, continuity equation becomes an algebraic equation and is eliminated from the system of governing equations with suitable modifications. We expect better pressure–velocity coupling in the present formulation compared to previous formulations which retain continuity equation. It has been shown by Pontaza [8] that pressure and velocities are not coupled strongly in previous least-squares formulations.

Bochev and Gunzburger [9] studied stress-based first-order system for the incompressible Stokes equations but retained continuity equation. They analysed weighted (mesh-dependent weights) as well as the unweighted L_2 least-squares functional. They showed that weighted least-squares formulation converges faster but suffers from the problem of bad conditioning of the coefficient matrix. They tested the formulation with several model problems. However, no detailed numerical results were reported.

Previous studies [10, 11] showed that mass conservation is not very good in least-squares-based formulations. Chang and Nelson [10] suggested that this is because the error is minimized on a global scale, allowing errors of significant size to remain on a local scale, especially in areas in which the gradients of the variables are of significant size. They also proposed a remedy. Unfortunately, this remedy, which consists of enforcing the continuity equation as an explicit constraint through the use of Lagrange multipliers, negates one of the main advantages of the least-squares methods, namely, the positive-definiteness of resulting coefficient matrix. Deang and Gunzburger [12] also studied mass conservation in least-squares formulations and analysed weighted least-squares functionals. These formulations have better mass conservation than un-weighted formulations but conditioning number of the resultant coefficient matrix becomes high. Bolton and Thatcher also addressed this problem for Stokes [11] and Navier–Stokes equations [13] and proposed weighting of particular terms in the least-squares functional. Pontaza and Reddy [5, 6] used high-order basis functions and they did not observe problems with mass conservation. However, for unsteady backward-facing problem numerical solutions become unstable if sufficiently high p-level was not used. In this study we pay particular attention to mass conservation and solve problems on relatively coarse meshes to check mass conservation. We examine mesh dependence of the solution for transient backward-facing step problem.

The paper is organized as follows. In Section 2, the stress-based least-squares finite-element model for the steady incompressible Navier–Stokes equations is presented. Numerical results are presented in Section 3. The h and p convergence are verified using the exact solution of the Kovasznay flow problem. First we present results for two-dimensional flow past a large circular cylinder in a channel. We check the dependence of mass conservation on mesh size. Next, numerical results are presented for the transient two-dimensional flow over a backward-facing step. We run the simulation for various meshes and report evolution of velocity field with time. We compare these results with the results obtained using traditional vorticity–pressure formulation. We conclude the paper with some remarks.

DOI: 10.1002/fld

2. THE INCOMPRESSIBLE NAVIER–STOKES EQUATIONS

Notation

Let Ω denote an open-bounded domain in $\mathbb{R}^n$, $n=2$ or 3, having a sufficiently smooth boundary Γ. Throughout this paper, vectors will be denoted by boldface letters, e.g. $\mathbf{u}$, and tensors by underlined boldface capitals, e.g. $\underline{\mathbf{T}}$. We use the standard notation and definition for the Sobolev spaces $H^s(\Omega)$ and $H^s(\Gamma)$, $s \geqslant 0$, with corresponding inner products denoted by $(\cdot,\cdot)_{s,\Omega}$ and $(\cdot,\cdot)_{s,\Gamma}$. By $\mathbf{H}^s(\Omega)$ we denote the product space $[H^s(\Omega)]^n$; and $H_0^1(\Omega)$ denotes the space of functions from $H^1(\Omega)$ that vanish on the boundary Γ.

The steady incompressible Navier–Stokes equations in dimensionless form can be written as

$$\nabla \cdot \mathbf{u} = 0 \quad \text{in } \Omega \tag{1}$$

$$(\mathbf{u}\cdot\nabla)\mathbf{u} + \nabla p - \frac{1}{Re}\nabla\cdot[(\nabla\mathbf{u}) + (\nabla\mathbf{u})^{\mathrm{T}}] = \mathbf{f} \quad \text{in } \Omega \tag{2}$$

$$\mathbf{u} = \mathbf{u}^{\mathrm{s}} \quad \text{on } \Gamma_{\mathrm{u}} \tag{3}$$

$$\hat{\mathbf{n}}\cdot\underline{\boldsymbol{\sigma}} = \mathbf{f}^{\mathrm{s}} \quad \text{on } \Gamma_{\mathrm{f}} \tag{4}$$

where $\mathbf{u}(\mathbf{x})$ is the velocity vector, $\underline{\boldsymbol{\sigma}} = -p\underline{\mathbf{I}} + 1/Re[(\nabla\mathbf{u}) + (\nabla\mathbf{u})^{\mathrm{T}}]$ is the total stress, $p(\mathbf{x})$ is the pressure, $\mathbf{f}$ is a dimensionless force, $\hat{\mathbf{n}}$ is the outward unit normal on the boundary of Ω, $\mathbf{u}^{\mathrm{s}}$ is the prescribed velocity on the boundary Γ_{u}, and $\mathbf{f}^{\mathrm{s}}$ are the prescribed tractions on the boundary Γ_{f}, $\Gamma = \Gamma_{\mathrm{u}} \cup \Gamma_{\mathrm{f}}$ and $\Gamma_{\mathrm{u}} \cap \Gamma_{\mathrm{f}} = \emptyset$, and Re is the Reynolds number.

2.1. The stress-based first-order system

To define the first-order velocity–pressure–stress system, 'scaled' stress tensor (symmetric part of velocity gradient tensor) is introduced

$$\underline{\mathbf{T}} = [(\nabla\mathbf{u}) + (\nabla\mathbf{u})^{\mathrm{T}}] \tag{5}$$

Then Equations (1)–(4) can be replaced by an equivalent system of first-order equations. The problem now can be stated as one of finding the velocity vector $\mathbf{u}(\mathbf{x})$, pressure $p(x)$ and stress tensor $\underline{\mathbf{T}}(\mathbf{x})$ such that

$$\nabla \cdot \mathbf{u} = 0 \quad \text{in } \Omega \tag{6}$$

$$(\mathbf{u}\cdot\nabla)\mathbf{u} + \nabla p - \frac{1}{Re}\nabla\cdot\underline{\mathbf{T}} = \mathbf{f} \quad \text{in } \Omega \tag{7}$$

$$\underline{\mathbf{T}} - [(\nabla\mathbf{u}) + (\nabla\mathbf{u})^{\mathrm{T}}] = \underline{\mathbf{0}} \quad \text{in } \Omega \tag{8}$$

$$\mathbf{u} = \mathbf{u}^{\mathrm{s}} \quad \text{on } \Gamma_{\mathrm{u}} \tag{9}$$

$$\hat{\mathbf{n}}\cdot\underline{\mathbf{T}} = \mathbf{T}^{\mathrm{s}} \quad \text{on } \Gamma_T \tag{10}$$

In component form these equations can be written as

$$\frac{\partial u}{\partial x} + \frac{\partial v}{\partial y} = 0 \quad \text{in } \Omega \tag{11}$$

DOI: 10.1002/fld

$$u\frac{\partial u}{\partial x}+v\frac{\partial u}{\partial y}+\frac{\partial p}{\partial x}-\frac{1}{Re}\left[\frac{\partial T_{xx}}{\partial x}+\frac{\partial T_{xy}}{\partial y}\right]=0 \quad \text{in } \Omega \tag{12}$$

$$u\frac{\partial v}{\partial x}+v\frac{\partial v}{\partial y}+\frac{\partial p}{\partial y}-\frac{1}{Re}\left[\frac{\partial T_{xy}}{\partial x}+\frac{\partial T_{yy}}{\partial y}\right]=0 \quad \text{in } \Omega \tag{13}$$

$$T_{xx}-2\frac{\partial u}{\partial x}=0 \quad \text{in } \Omega \tag{14}$$

$$T_{xy}-\frac{\partial u}{\partial y}-\frac{\partial v}{\partial x}=0 \quad \text{in } \Omega \tag{15}$$

$$T_{yy}-2\frac{\partial v}{\partial y}=0 \quad \text{in } \Omega \tag{16}$$

$$\mathbf{u}=\mathbf{u}^{\mathrm{s}} \quad \text{on } \Gamma_{\mathrm{u}} \tag{17}$$

$$\hat{\mathbf{n}}\cdot\underline{\mathbf{T}}=\mathbf{T}^{\mathrm{s}} \quad \text{on } \Gamma_T \tag{18}$$

Continuity equation can be written as

$$\frac{\partial u}{\partial x}+\frac{\partial v}{\partial y}=0 \quad \text{in } \Omega \tag{19}$$

$$\Rightarrow \quad T_{xx}=-T_{yy} \quad \text{in } \Omega \tag{20}$$

Continuity equation is eliminated and T_{yy} is replaced by $-T_{xx}$ in the system of governing equations. Then Navier–Stokes and continuity equations can be replaced by an equivalent system of first-order equations. The problem now can be stated as one of finding the velocity vector $\mathbf{u}(\mathbf{x})$ pressure $p(\mathbf{x})$ and stress tensor components T_{xx}, T_{xy} such that

$$u\frac{\partial u}{\partial x}+v\frac{\partial u}{\partial y}+\frac{\partial p}{\partial x}-\frac{1}{Re}\left[\frac{\partial T_{xx}}{\partial x}+\frac{\partial T_{xy}}{\partial y}\right]=0 \quad \text{in } \Omega \tag{21}$$

$$u\frac{\partial v}{\partial x}+v\frac{\partial v}{\partial y}+\frac{\partial p}{\partial y}-\frac{1}{Re}\left[\frac{\partial T_{xy}}{\partial x}-\frac{\partial T_{xx}}{\partial y}\right]=0 \quad \text{in } \Omega \tag{22}$$

$$T_{xx}-2\frac{\partial u}{\partial x}=0 \quad \text{in } \Omega \tag{23}$$

$$T_{xy}-\frac{\partial u}{\partial y}-\frac{\partial v}{\partial x}=0 \quad \text{in } \Omega \tag{24}$$

$$-T_{xx}-2\frac{\partial v}{\partial y}=0 \quad \text{in } \Omega \tag{25}$$

$$\mathbf{u}=\mathbf{u}^{\mathrm{s}} \quad \text{on } \Gamma_{\mathrm{u}} \tag{26}$$

$$\hat{\mathbf{n}}\cdot\underline{\mathbf{T}}=\mathbf{T}^{\mathrm{s}} \quad \text{on } \Gamma_T \tag{27}$$

DOI: 10.1002/fld

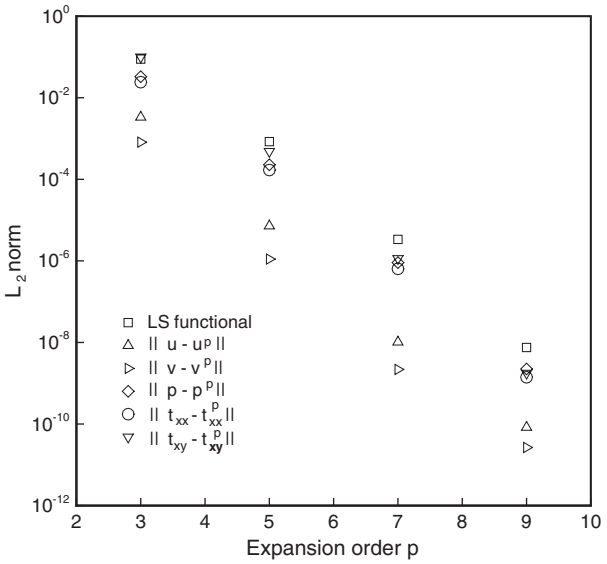

Figure 1. Convergence of the least-squares functional, velocity, pressure and stress field to the exact Kovasznay solution: p-convergence.

2.1.1. L_2 least-squares formulation. The least-squares functional of the problem can be set up by summing up the squares of the residual of the new set of equations

$$\mathscr{J}(\mathbf{u}, p, T_{xx}, T_{xy}; \mathbf{f}) = \tfrac{1}{2}(\|R_1\|_0^2 + \|R_2\|_0^2 + \|R_3\|_0^2 + \|R_4\|_0^2 + \|R_5\|_0^2) \tag{28}$$

where R_1–R_5 are the residuals of Equations (21)–(25).

Considering the homogeneous pure velocity boundary condition case, the least-squares principle for functional (28) can be stated as:
find the velocity vector $\mathbf{u}(\mathbf{x})$, pressure $p(x)$ and stress components T_{xx} and T_{xy} such that

$$\mathscr{J}(\mathbf{u}, p, T_{xx}, T_{xy}; \mathbf{f}) \leqslant \mathscr{J}(\tilde{\mathbf{u}}, \tilde{p}, \tilde{T_{xx}}, \tilde{T_{xy}}; \mathbf{f}) \quad \forall(\tilde{\mathbf{u}}, \tilde{p}, \tilde{T_{xx}}, \tilde{T_{xy}}) \in \mathbf{X} \tag{29}$$

where we use the space

$$\mathbf{X} = \{(\mathbf{u}, p, T_{xx}, T_{xy}) \in \mathbf{H}_0^1(\Omega) \times H^1(\Omega) \cap \bar{L}_2(\Omega) \times H^1(\Omega) \times H^1(\Omega)\}$$

The variational problem and finite-element model are constructed in conventional way, details of which can be found in [5].

We use space–time decoupled formulation where discretizations in space and time are done independently. The Crank–Nicholson scheme is used for time approximation.

DOI: 10.1002/fld

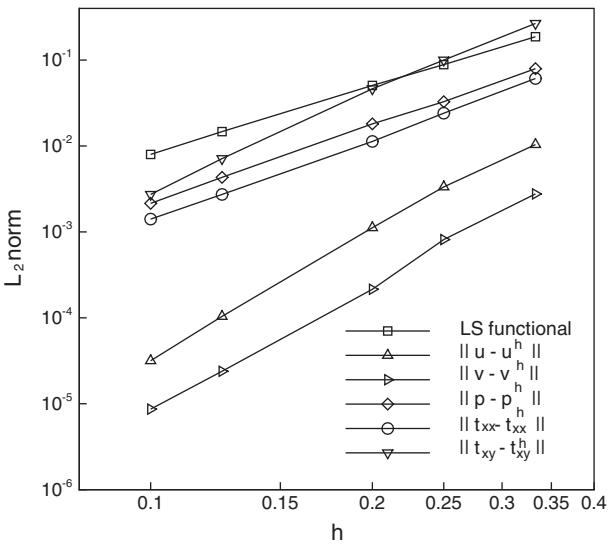

Figure 2. Convergence of the least-squares functional, velocity, pressure, and stress field to the exact Kovasznay solution: h-convergence.

2.1.2. Expansion bases. There is no compatibility condition, such as LBB condition, in this formulation, so all the variables are approximated using the same interpolation functions. We use low-order basis functions (*bilinear Lagrange basis functions*) in this study, except when we verify h and p convergence, we use high-order nodal expansion.

Nodal expansion
In the standard interval $\Omega_{\text{st}} = \{\xi | -1 < \xi < 1\}$ nodal expansions are defined as

$$\psi_i(\xi) = \frac{(\xi - 1)(\xi + 1)L'_p(\xi)}{p(p+1)L_p(\xi_i)(\xi - \xi_i)} \tag{30}$$

In Equation (30), $L_p = P_p^{0,0}$ is the Legendre polynomial of order p and ξ_i denotes the location of the roots of $(\xi - 1)(\xi + 1)L'_p(\xi) = 0$ in the interval $[-1, 1]$. Details on the multidimensional construction of nodal expansions can be found in Reference [14].

The integrals are evaluated using Gauss quadrature rules. In the computer implementation, one point Gauss quadrature is used for bilinear Lagrange basis functions and Gauss–Lobatto–Legendre rule is used for high-order basis functions. For details on standard finite-element computer implementation, such as mapping $\bar{\Omega}_e \rightleftarrows \hat{\Omega}_e$, numerical integration in $\hat{\Omega}_e$, and assembly using the direct stiffness approach, see Reddy [15, 16]. For linearization, we use Newton's method, details of which can be found in [17].

DOI: 10.1002/fld

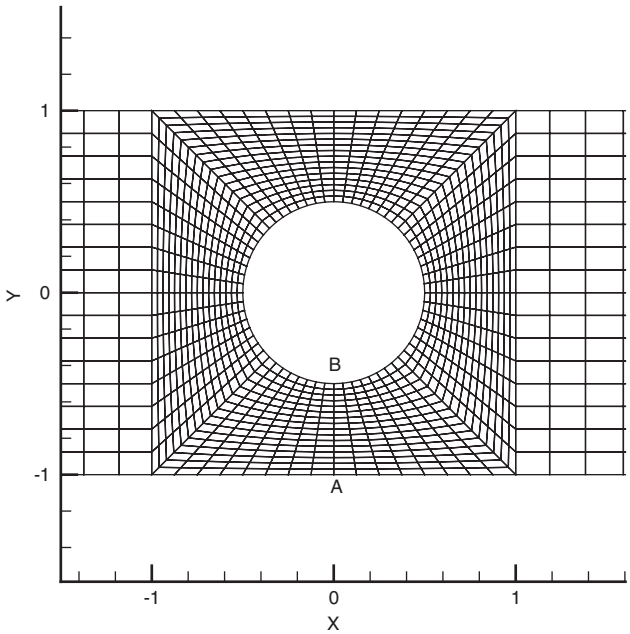

Figure 3. Close-up view of the geometric discretization around the cylinder.

2.2. *Implementation of boundary conditions*

In general, in a given problem we have boundary conditions on the primary variables and/or secondary (force) variables. Boundary conditions on the primary variables can be implemented easily in the strong sense by restricting the value of corresponding degree of freedom.

Boundary conditions on the secondary variables (typically, they involve derivatives of the primary variables) are imposed in a weak sense through the least-squares functional. For example, the outflow boundary condition, $\hat{\mathbf{n}}\cdot\tilde{\boldsymbol{\sigma}} = \hat{\mathbf{n}}\cdot(-p\mathbf{I}+(1/Re)\nabla\mathbf{u}) = 0$ which is equivalent to (at $x =$ constant boundary)

$$-p + \frac{1}{2\,Re}T_{xx} = 0 \tag{31}$$

and

$$\frac{1}{Re}\frac{\partial v}{\partial x} = 0 \tag{32}$$

is implemented by modifying the L_2 least-squares functional to be

$$\mathscr{J}(\mathbf{u},\, p,\, T_{xx},\, T_{xy};\, \mathbf{f}) = \frac{1}{2}\left(\|R_1\|_0^2 + \|R_2\|_0^2 + \|R_3\|_0^2 + \|R_4\|_0^2 + \|R_5\|_0^2 \right.$$
$$\left. + \left\| -p + \frac{1}{2\,Re}T_{xx} \right\|_{0,\Gamma_{\text{outflow}}}^2 + \left\| \frac{1}{Re}\frac{\partial v}{\partial x} \right\|_{0,\Gamma_{\text{outflow}}}^2 \right) \tag{33}$$

DOI: 10.1002/fld

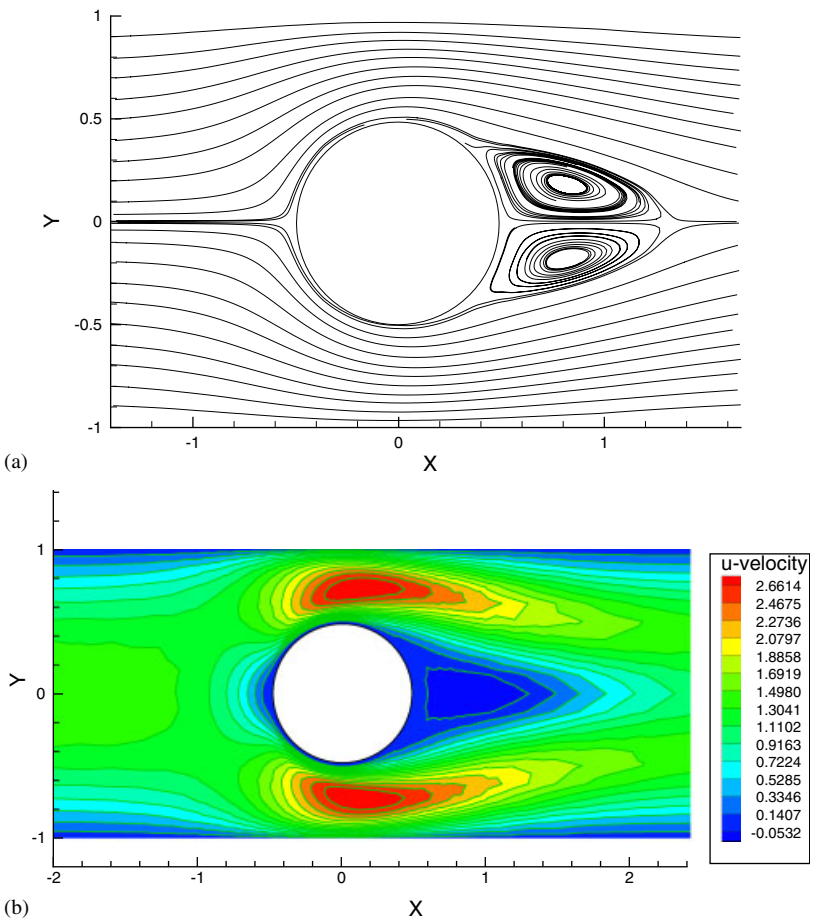

Figure 4. Flow past a large circular in a channel: (a) streamlines and (b) u-velocity contours.

3. NUMERICAL RESULTS

In this section, numerical results obtained with the present least-squares finite-element model are presented. First, h and p convergence of the proposed formulation are verified. Next, results are presented for steady flow past a circular cylinder and transient flow over a backward-facing step.

For all the problems considered in this paper, non-linear convergence is declared when the relative norm of the residual, $\|\Delta\mathbf{U}\|/\|\mathbf{U}\|$ is less than 10^{-3} unless mentioned, where $\mathbf{U}$ is the solution vector (includes all degrees of freedom at a node). Convergence of conjugate gradient is declared when L_2-norm of error is less than 10^{-6}. In this study we use Jacobi preconditioner as only diagonal entries of coefficient matrix are needed to be stored as opposed to other preconditioners which require partial or full coefficient matrix.

DOI: 10.1002/fld

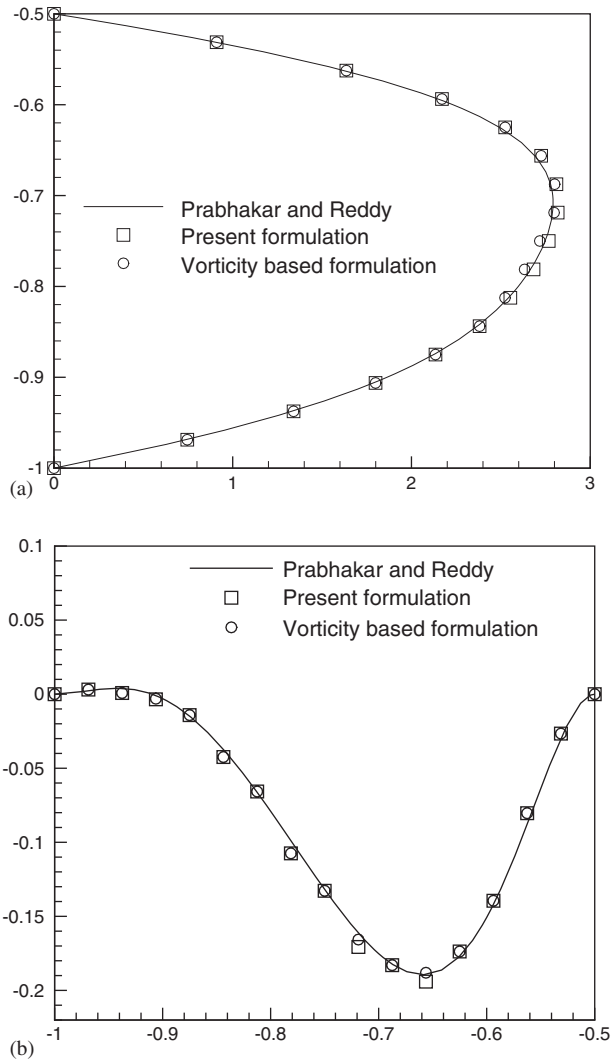

Figure 5. (a) Variation of u-velocity along AB and (b) variation of v-velocity along AB (for Mesh 1).

3.1. Verification problem: Kovasznay flow

The benchmark problem to be used for the purpose of verification of the least-squares-based finite-element model is an analytical solution to the two-dimensional steady incompressible Navier–Stokes due to Kovasznay [18]. Domain of interest is $\bar{\Omega} = [-0.5, 1.5] \times [-0.5, 1.5]$. The solution is given by

$$u = 1 - \mathrm{e}^{\lambda x} \cos(2\pi y) \tag{34}$$

DOI: 10.1002/fld

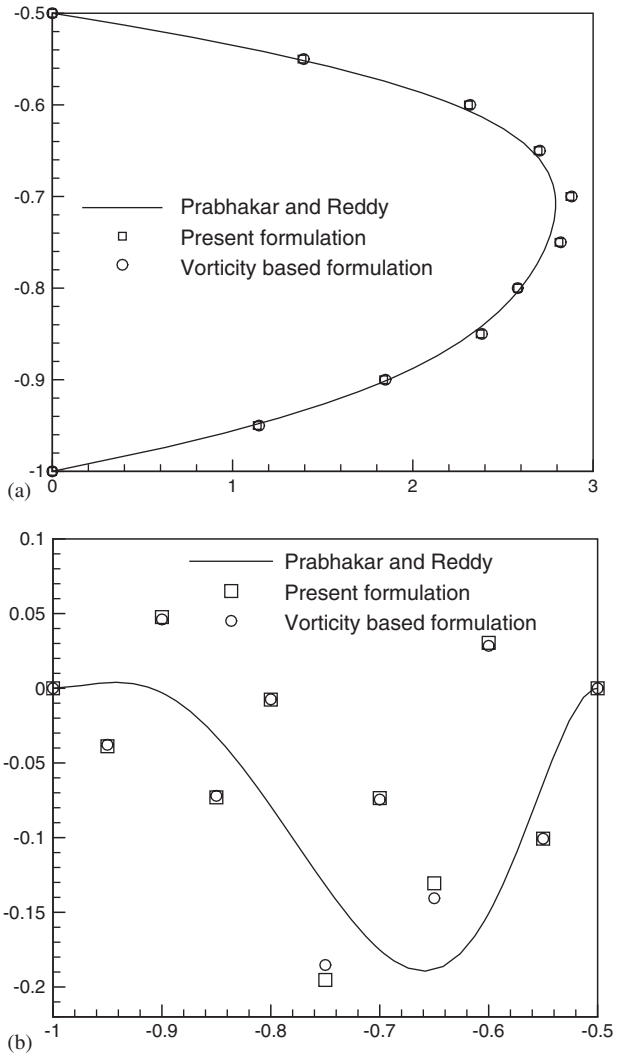

Figure 6. (a) Variation of u-velocity along AB and (b) variation of v-velocity along AB (for Mesh 2).

$$v = \frac{\lambda}{2\pi} e^{\lambda x} \sin(2\pi y) \tag{35}$$

$$p = p_0 - \tfrac{1}{2} e^{2\lambda x} \tag{36}$$

where $\lambda = Re/2 - [(Re^2/4) + 4\pi^2]^{1/2}$ and p_0 is a reference pressure (an arbitrary constant).

Dirichlet boundary conditions on velocities are specified using the exact solution given by Equations (34) and (35). The discrete system is linearized using Newton's method, and resulting SPD system of equations has been solved using PCG solver. Newton's convergence is declared

DOI: 10.1002/fld

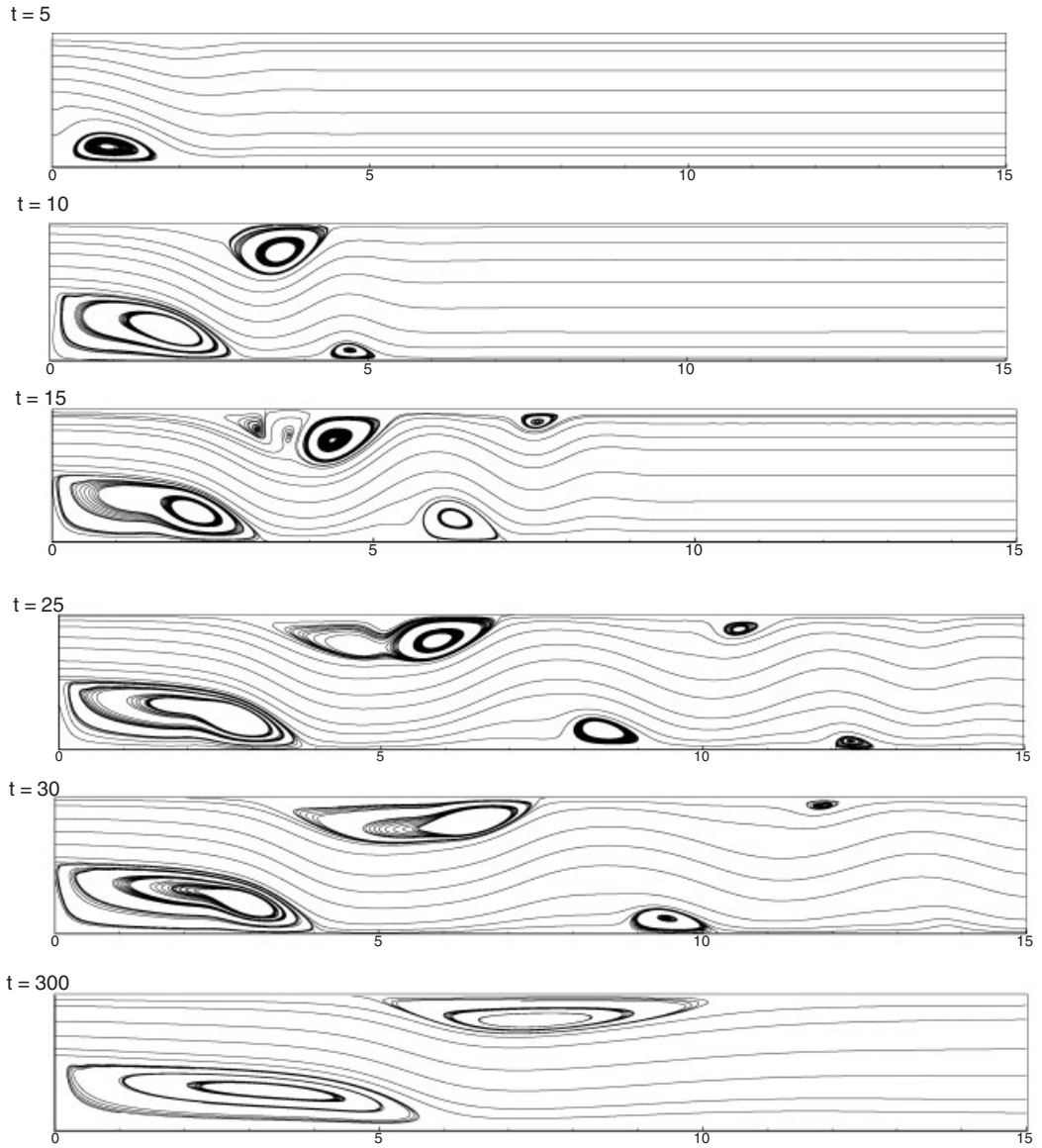

Figure 7. Time history of streamline plots for low over a backward-facing step.

when the relative norm of the residual is less than 10^{-10}. Convergence of conjugate gradient is declared when L_2-norm of error is less than 10^{-10}.

An 8×8 uniform mesh is used. To verify spectral convergence (p-convergence), L_2-norm of least-square functional $\mathscr{J}$ and L_2 error of the velocity, pressure and stress fields are plotted against polynomial order in Figure 1. On logarithmic linear scale we obtain almost straight line for all the variables verifying exponential decay with respect to the polynomial degree used.

DOI: 10.1002/fld

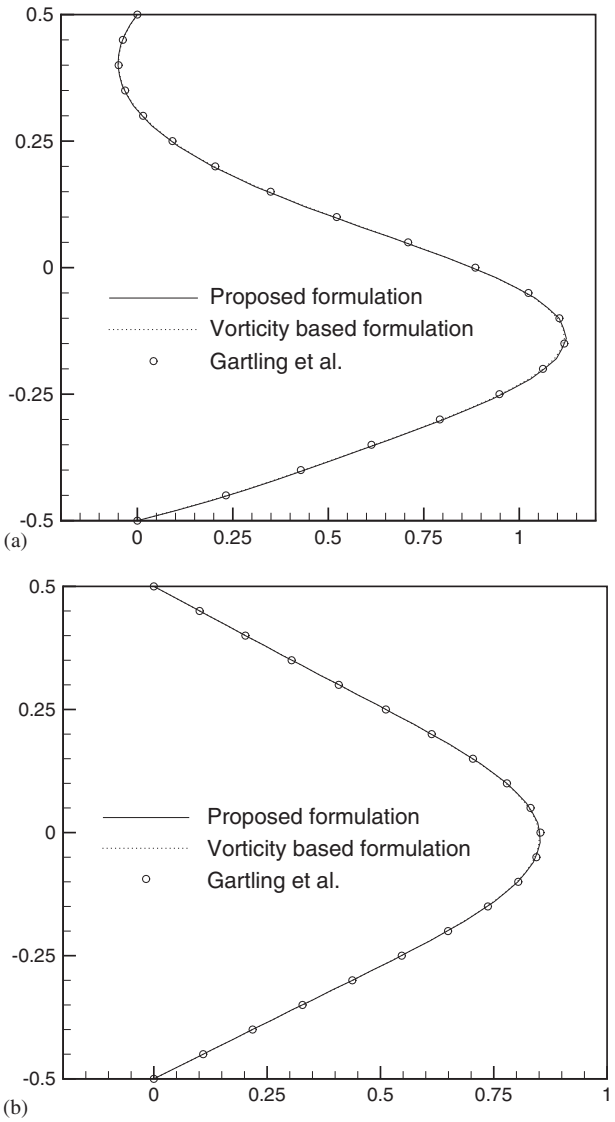

Figure 8. Horizontal velocity profile along the height of the channel at: (a) $x = 7$ and (b) $x = 15$: Mesh A.

Next, we perform an h-refinement study. For such a study, we fix the p-level of the element approximation functions ($P = 3$), and systematically refine the mesh. The error measures should decay at an algebraic rate as the mesh is refined. On a log–log scale it should be a straight line. Five different uniform meshes are used to perform the h-refinement study. The meshes are varied successively from 6×6 to 20×20. In Figure 2 L_2-norm of least-square functional $\mathscr{J}$ and L_2 error of the velocity, pressure and stress fields are plotted against h. An algebraic convergence rate slightly better than 4 is achieved by u, v and T_{xy} and slightly better than 3 is achieved by p, T_{xx} and L_2-norm of least-squares functional.

DOI: 10.1002/fld

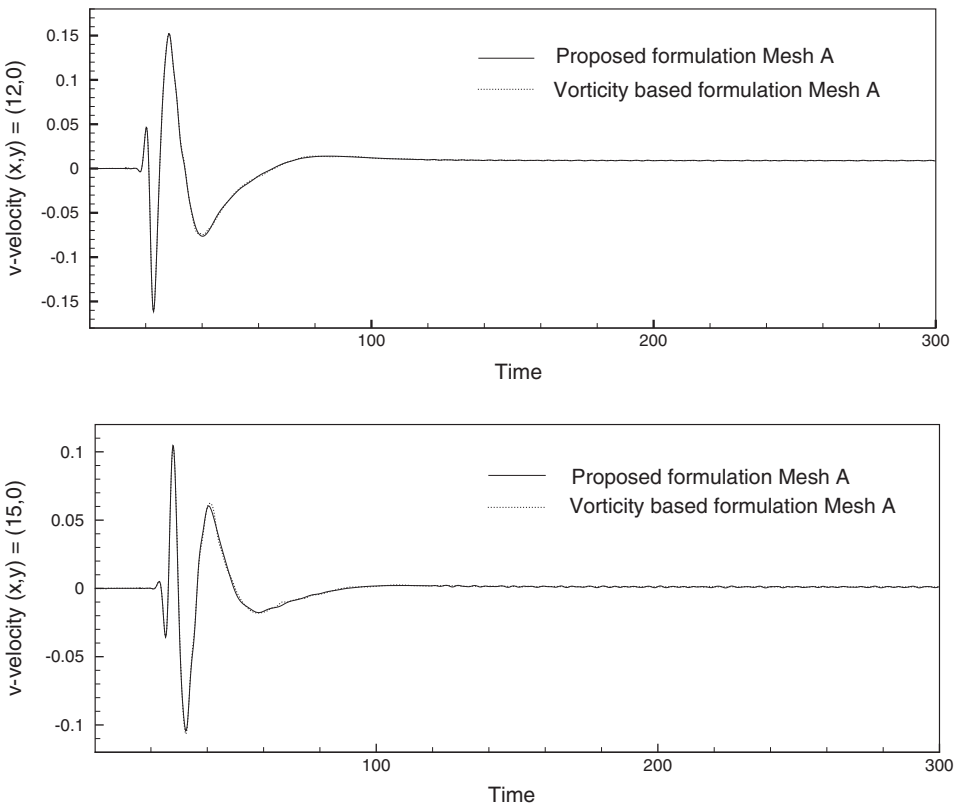

Figure 9. Time history of the v-velocity component at two selected locations: Mesh A.

3.2. Flow past a large circular cylinder in a channel

To test mass conservation rigorously, we solve flow past a large circular cylinder in a channel with blockage ratio of 2 ($H/D=2$). Chang and Nelson [10] used similar problem to test mass conservation for Stokes flow. Domain of interest is $[-10.0, 15.0]\times[-1.0, 1.0]$. Cylinder has unit diameter and it is centred at (0.0, 0.0). No-slip boundary conditions are imposed on side walls. At inlet boundary conditions are $u=1.0$ and $v=0.0$. The outflow boundary conditions are imposed in a weak sense through the least-squares functional. Reynolds number considered here is 40 for which steady-state solution exists.

Figure 3 contains a close-up view of the geometric discretization around the circular cylinder. We use quadrilateral elements. There are 1824 elements in the mesh and 1938 nodes (Mesh 1). Figure 4(a) shows streamline plot. In this case separation delayed. u-velocity contours around the cylinder are shown in Figure 4(b). The predicted wake extends 1.68 cylinder radius measured from the back of the cylinder.

Next, u- and v-velocities are plotted along line AB (see Figure 3) for both stress-based and vorticity-based formulations. Present results are compared with the results of Prabhakar and Reddy [7] who solved the same problem using spectral/hp penalty least-squares formulation. Results in [7] are expected to be accurate to a good extent. Present results match well with the

DOI: 10.1002/fld

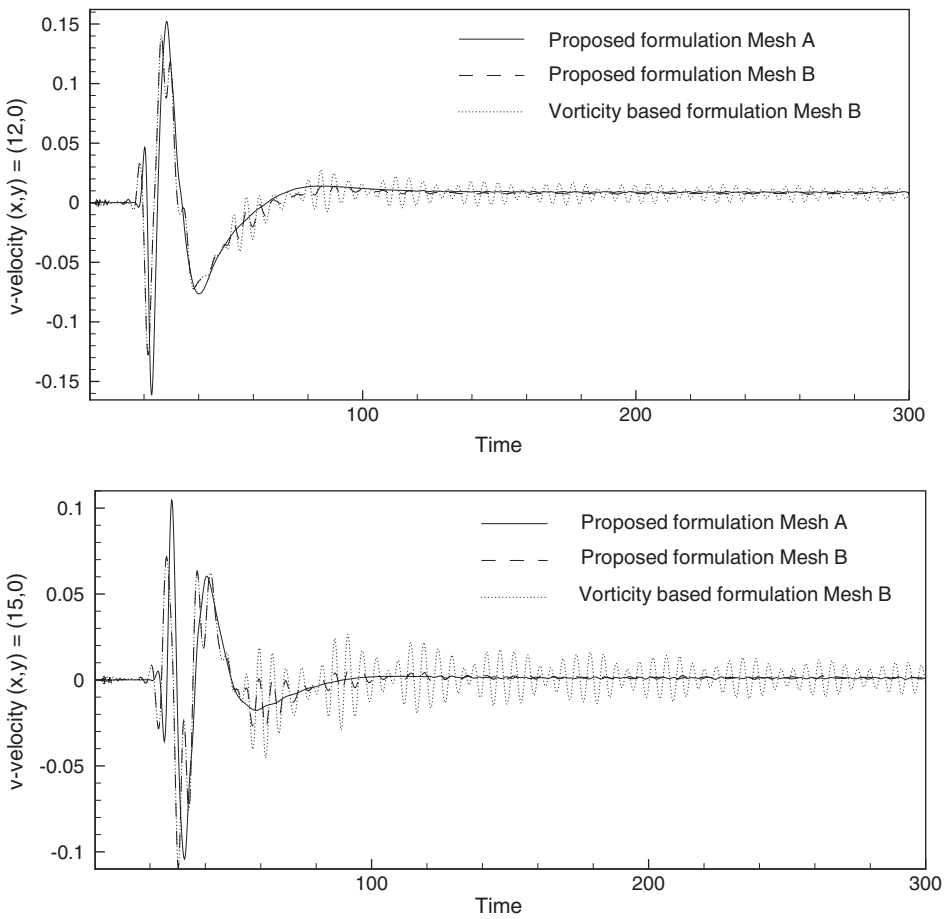

Figure 10. Time history of the v-velocity component at two selected locations: Mesh B.

results of Prabhakar and Reddy [7]. Mass flow rate at $x = 0$ is calculated and found to be 1.98 for stress-based and vorticity-based formulations (Figure 5).

Next we coarsen the mesh. We generate a similar mesh shown in Figure 3 with 720 elements and 802 nodes (Mesh 2); u and v-velocities are plotted along line AB (see Figure 6) and compared with the results obtained with hp penalty least-squares formulation. While u-velocity profile matches to a good extent, v-velocities are significantly off. On coarse mesh both formulations produce 'equally inaccurate' results.

3.3. Transient flow over a backward-facing step

Next, we consider two-dimensional transient flow over a backward-facing step at $Re = 800$. The domain of interest is $\bar{\Omega} = [0, 30] \times [-0.5, 0.5]$. The boundary and initial conditions used here are those used in the work of Gresho *et al.* [19] and Pontaza and Reddy [6]: $u = v = 0$ on the horizontal walls, $-p + \mu \partial u/\partial n = 0$ and $\partial v/\partial n = 0$ on the outflow boundary, and $u = [\tanh(t/4)]u_b(y) +$

DOI: 10.1002/fld

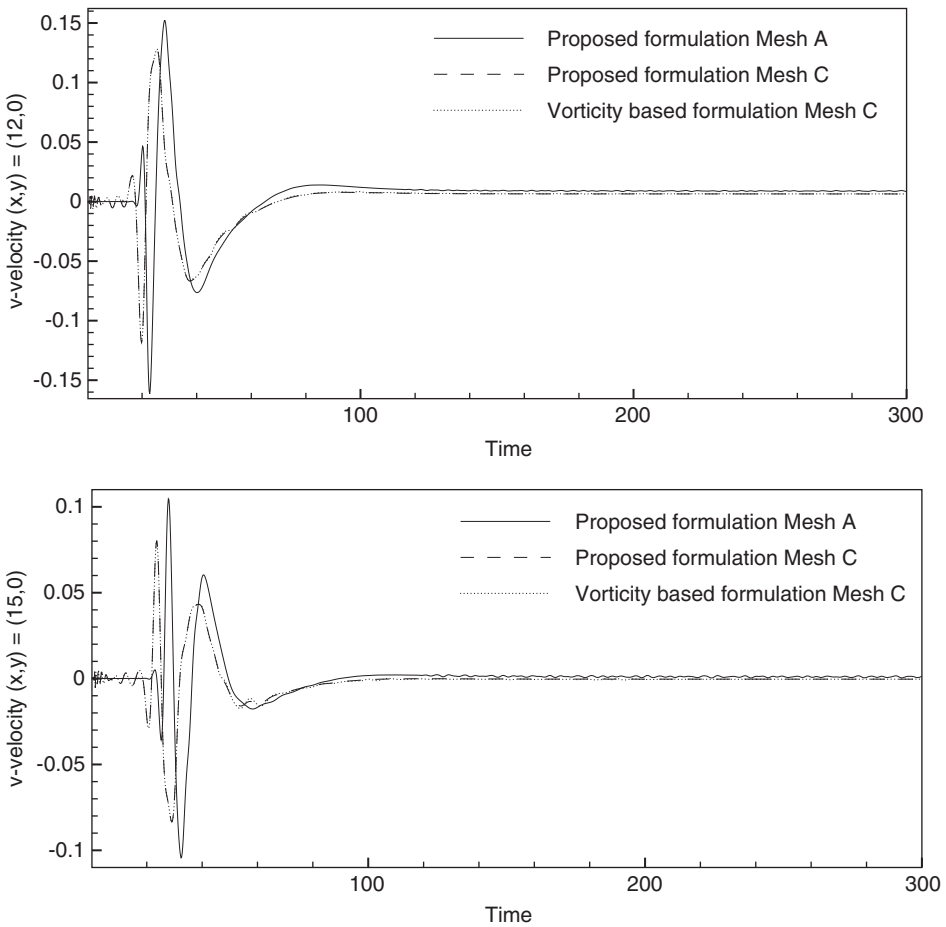

Figure 11. Time history of the v-velocity component at two selected locations: Mesh C.

$[1 - \tanh(t/4)]u_p(y)$ and $v = 0$ on the inflow boundary. Here $u_b(y) = \max[0, 24y(0.5 - y)]$ is the true inlet boundary condition and $u_p(y) = 3(0.5 - y)(0.5 + y)$ is the Poiseuille flow observed infinitely far downstream at steady flow conditions. The initial velocity field is set to $u = u_p(y)$ and $v = 0$ everywhere in the computational domain. The inlet condition is varied fast but smoothly from Poiseuille flow to flow over a backward-facing step.

A 150×50 mesh has been used. Along the x direction, there are 90 uniform elements till $x = 15$ and 60 uniform elements from $x = 15$ to $x = 30$. Mesh is uniform in the y direction. The Crank–Nicholson scheme is used for time marching, and a time increment of $\Delta t = 0.2$ has been used for all the results reported in this section.

Figure 7 shows the evolution of the flow field. The main flow coming from the inlet follows a sinuous path, forming a series of eddies along the upper and lower walls. At steady state, two eddies (primary and secondary separation zones) remain, all other eddies die out. These plots match qualitatively well with the published result of Pontaza and Reddy [6]. In the steady state,

DOI: 10.1002/fld

the primary reattachment length is around 6.10, while secondary separation and reattachment lengths are approximately 4.9 and 10.4, respectively. These values match well with the benchmark results [20]. The u-velocity profiles along the channel height at $x = 7$ and 15 are compared with the benchmark results of Gartling [20] in Figure 8 (steady-state profile). Excellent agreement is found. This problem is also solved using vorticity-based first-order least-squares finite-element method under the same conditions. Figure 9 shows the time history of the v-velocity component at two locations along the channel's mid-section for stress-based and vorticity-based first-order formulations. Both formulations predict same velocity evolution. There are no fluctuations in v-velocity signal showing that mesh resolution is adequate.

Previous work of Gresho *et al.* [19], Torczynski [21] and Pontaza and Reddy [6] showed that lack of spatial resolution induces unrealistic temporal chaotic behaviour resulting in an erroneous prediction of the long-term behaviour of the flow. In such cases either simulation diverges or the velocities fluctuate with time if it converges to steady state [6]. We coarsen the mesh and solve this problem on 60×20 (40+20 in the x direction) and 40×16 mesh (25+15 in the x direction). These meshes are uniform in the y direction. Figure 10 shows time history of v-velocity at two locations for both stress-based and vorticity-based formulations for 60×20 mesh. Stress-based formulation does not show much sensitivity towards mesh coarsening and for 60×20 grid results are close to that for 150×50. Vorticity-based formulation shows pronounced fluctuation in v-velocity. However, simulation does not diverge.

On 40×16 mesh, v-velocity evolutions are the same for both the formulations but significantly off from accurate results on 150×50 mesh (Figure 11). Steady state is achieved in these simulations.

4. CONCLUDING REMARKS

In this paper we presented a stress-based least-squares finite-element formulation for the solution of incompressible Navier–Stokes equations. Stress components were introduced as independent variables to make the system first order. Continuity equation became an algebraic equation and was eliminated from the system with suitable modifications. This formulation carries one less degree of freedom compared to existing stress-based first-order formulations [9]. The h and p convergence were verified using the exact solution of Kovasznay flow. Steady flow past a large circular cylinder in a channel is solved to check mass conservation and we found good mass conservation. Transient flow over a backward-facing problem was solved on three different meshes and accuracy was investigated. We compared results obtained by proposed formulation with that obtained by vorticity-based formulation and found that proposed formulation was less affected with mesh coarsening.

ACKNOWLEDGEMENTS

The authors gratefully acknowledge the support of this work by the Computational Mathematics Program of the Air Force Office of Scientific Research through Grant F49620-03-1-0201 and Structural Dynamics Program of Army Research Office through Grant 45508-EG.

REFERENCES

1. Jiang BN. On the least-squares method. *Computer Methods in Applied Mechanics and Engineering* 1997; **152**:239–257.

DOI: 10.1002/fld

2. Jiang BN. *The Least-Squares Finite Element Method* (1st edn). Springer: Berlin, 1998.
3. Bochev PV, Gunzburger MD. Finite element methods of least-squares type. *SIAM Review* 1998; **40**:789–837.
4. Proot MMJ, Gerritsma MI. Least-squares spectral elements applied to the Stokes problem. *Journal of Computational Physics* 2002; **181**:454–477.
5. Pontaza JP, Reddy JN. Spectral/*hp* least-squares finite element formulation for the Navier–Stokes equations. *Journal of Computational Physics* 2003; **190**:523–549.
6. Pontaza JP, Reddy JN. Space–time coupled spectral/*hp* least-squares finite element formulation for the incompressible Navier–Stokes equations. *Journal of Computational Physics* 2004; **197**:418–459.
7. Prabhakar V, Reddy JN. Spectral/*hp* penalty least-squares finite element formulation for the steady incompressible Navier–Stokes equations. *Journal of Computational Physics* 2006; **215**:274–297.
8. Pontaza JP. A least-squares finite element formulation for the unsteady incompressible flows with improved velocity–pressure coupling. *Journal of Computational Physics* 2006; **217**:563–588.
9. Bochev PV, Gunzburger MD. Least-squares methods for the velocity–pressure–stress formulation of the Stokes equations. *Computer Methods in Applied Mechanics and Engineering* 1995; **126**:267–287.
10. Chang CL, Nelson JJ. Least-squares finite element method for the Stokes problem with zero residual of mass conservation. *SIAM Journal on Numerical Analysis* 1997; **34**:480–489.
11. Bolton P, Thatcher RW. On mass conservation in least-squares methods. *Journal of Computational Physics* 2005; **203**:287–304.
12. Deang JM, Gunzburger MD. Issues related to least-squares finite element methods for the Stokes equations. *SIAM Journal on Scientific Computing* 1998; **20**:878–906.
13. Bolton P, Thatcher RW. A least-squares finite element method for the Navier–Stokes equations. *Journal of Computational Physics* 2006; **213**:174–183.
14. Karniadakis GE, Sherwin SJ. *Spectral/hp Element Methods for CFD*. Oxford University Press: Oxford, 1999.
15. Reddy JN. *An Introduction to the Finite Element Method* (3rd edn). McGraw-Hill: New York, 2006.
16. Reddy JN. *Introduction to Nonlinear Finite Element Analysis*. Oxford University Press: Oxford, 2004.
17. Bell BC, Surana KS. A space–time coupled *p*-version least squares finite element formulation for unsteady two-dimensional Navier–Stokes equations. *International Journal for Numerical Methods in Engineering* 1996; **39**:2593–2618.
18. Kovasznay LSG. Laminar flow behind a two-dimensional grid. *Mathematical Proceedings of the Cambridge Philosophical Society* 1948; **44**:58–62.
19. Gresho PM, Gartling DK, Torczynski JR, Cliffe KA, Winters KH, Garrat TJ, Spence A, Goodrich JW. Is the steady viscous incompressible two-dimensional flow over a backward-facing step at $Re = 800$ stable? *International Journal for Numerical Methods in Fluids* 1993; **17**:501–541.
20. Gartling DK. A test problem for outflow boundary conditions—flow over a backward-facing step. *International Journal for Numerical Methods in Fluids* 1990; **11**:953–967.
21. Torczynski JR. A grid refinement study of two-dimensional transient flow over a backward-facing step using a spectral element method. In *Separated Flows*, Duuton JC, Purtell LP (eds), vol. 149. ASME: New York, 1993; 44–62.

DOI: 10.1002/fld